2011773, 2022, 10. Downloaded from https://onlinelibrary.wiley.com/doi/10.1002/anie.202116897, Wiley Online Library on [29/11/2022]. See the Terms and Conditions (https://onlinelibrary.wiley.com/terms-and-conditions) on Wiley Online Library for rules of use; OA articles are governed by the applicable Creative Commons Licensee the Terms and Conditions (https://onlinelibrary.wiley.com/terms-and-conditions) on Wiley Online Library for rules of use; OA articles are governed by the applicable Creative Commons Licensee the Terms and Conditions (https://onlinelibrary.wiley.com/terms-and-conditions) on Wiley Online Library for rules of use; OA articles are governed by the applicable Creative Commons Licensee the Terms and Conditions (https://onlinelibrary.wiley.com/terms-and-conditions) on Wiley Online Library for rules of use; OA articles are governed by the applicable Creative Commons Licensee the Terms and Conditions (https://onlinelibrary.wiley.com/terms-and-conditions) on Wiley Online Library for rules of use; OA articles are governed by the applicable Creative Commons Licensee the Commo

Rotaxanes

How to cite: *Angew. Chem. Int. Ed.* **2022,** *61,* e202116897 International Edition: doi.org/10.1002/anie.202116897 German Edition: doi.org/10.1002/ange.202116897

Polyyne [3]Rotaxanes: Synthesis via Dicobalt Carbonyl Complexes and Enhanced Stability

Connor W. Patrick, Joseph F. Woods, Przemyslaw Gawel, Claire E. Otteson, Amber L. Thompson, Tim D. W. Claridge, Ramesh Jasti, and Harry L. Anderson*

Abstract: New strategies for synthesizing polyyne polyrotaxanes are being developed as an approach to stable carbyne "insulated molecular wires". Here we report an active metal template route to polyyne [3]rotaxanes, using dicobalt carbonyl masked alkyne equivalents. We synthesized two [3]rotaxanes, both with the same C_{28} polyyne dumbbell component, one with a phenanthroline-based macrocycle and one using a 2,6-pyridyl cycloparaphenylene nanohoop. The thermal stabilities of the two rotaxanes were compared with that of the naked polyyne dumbbell in decalin at 80° C, and the nanohoop rotaxane was found to be 4.5 times more stable

Reactive π -systems can be stabilized by threading them through protective macrocycles to generate rotaxanes or polyrotaxanes, as "insulated molecular wires".[1] This concept has been used to enhance the properties of many organic semiconductors and dyes.[1-3] One of the most interesting π -systems to select for stabilization in this way is carbyne, the 1D sp-hybridized allotrope of carbon, [4] because it seems unlikely that carbyne can exist as a pure carbon allotrope without some type of supramolecular encapsulation.^[5] Bulky terminal groups stabilize polyynes (i.e. oligomers of carbyne) with up to 24 contiguous alkyne units, [6] but stabilization from the end groups is expected to diminish with increasing chain length, whereas polyrotaxane formation could stabilize polyvnes of any length, making it possible to study the properties of long carbyne chains in solution. [2]Rotaxanes consisting of a single macrocycle threaded on a polyyne dumbbell are readily prepared using active metal templates; [7-10] the challenge is to synthesize long polyynes with many threaded macrocycles. One potential solution to this problem is to use bulky masked

[*] C. W. Patrick, J. F. Woods, Dr. P. Gawel, Dr. A. L. Thompson, Prof. T. D. W. Claridge, Prof. H. L. Anderson Department of Chemistry, University of Oxford Chemistry Research Laboratory, Oxford OX1 3TA (UK) E-mail: harry.anderson@chem.ox.ac.uk

C. E. Otteson, Prof. R. Jasti Department of Chemistry and Biochemistry Materials Science Institute, University of Oregon Eugene, OR 97403 (USA)

© 2022 The Authors. Angewandte Chemie International Edition published by Wiley-VCH GmbH. This is an open access article under the terms of the Creative Commons Attribution License, which permits use, distribution and reproduction in any medium, provided the original work is properly cited. alkyne equivalents (MAEs) which can subsequently be converted into alkynes, and which act as stoppers on a rotaxane intermediate. [9] Rotaxanes with MAE stoppers are promising precursors to carbyne polyrotaxanes and cyclocarbon catenanes. [9] Previously, we and others have investigated dicobalt carbonyl complexes as MAEs, [11,12] but attempts at synthesizing rotaxanes with these stoppers were unsuccessful. [11] Here we report the first synthesis of polyyne rotaxanes with dicobalt carbonyl MAE stoppers and the conversion of these [2] rotaxanes to polyyne [3] rotaxanes with 14 contiguous alkyne units, $1 \cdot (M1)_2$ and $1 \cdot (M2)_2$ (Scheme 1). We also report the enhanced thermal stability of the [3] rotaxane $1 \cdot (M2)_2$, compared with the corresponding C_{28} dumbbell.

Two [3]rotaxanes were targeted in this study: one based on a larger phenanthroline macrocycle M1, pioneered by Saito, [7a] and the other using a smaller 2,6-pyridyl cycloparaphenylene (nanohoop) M2, developed by Jasti and coworkers. [10] Many rotaxanes have been reported based on the Saito macrocycle M1, but molecular models indicate that it is too large and flexible to provide effective protection of a threaded polyyne. Crystal structures of rotaxanes based on M1 also show that the 2,9-diarylphenanthroline tends to form stacked aggregates, [13] which could reduce the screening of the polyyne thread in these [3]rotaxanes. In contrast, the nanohoop is expected to provide better shielding of the polyyne.

The synthesis of the [3]rotaxanes starts from terminal alkyne 2 (Scheme 1), which is readily available from TMS-C₆-TIPS, [14] as reported previously. [11] Active metal-template Cadiot-Chodkiewicz cross coupling of 2 with supertrityl bromo-triyne 3 in the presence of macrocycles M1 or M2 gave the [2]rotaxanes 4·M1 and 4·M2, although it was necessary to optimize the reaction conditions for each macrocycle. With the phenanthroline macrocycle, the M1·CuI complex was pre-formed and cross coupling was carried out in THF, with K₂CO₃ as the base, as previously reported, [8c,9b,15] to give [2]rotaxane 4·M1 in 35% isolated yield. In contrast, the nanohoop M2 did not form the target [2]rotaxane 4·M2 under these conditions; instead, only the non-interlocked dumbbell 4 was produced, presumably because its pyridine unit does not bind strongly enough to copper(I) cations in coordinating solvents such as THF. Changing to a non-coordinating solvent (CHCl₃), with diisopropylethylamine as the base^[10,16] afforded the desired [2]rotaxane 4·M2 in 43 % yield. Crystals of 4·M1 suitable for single-crystal X-ray diffraction^[17] were grown by layered addition of methanol to a solution in dichloromethane,

Scheme 1. Synthesis of the polyyne [3] rotaxanes 1. (M1)₂ and 1. (M2)₂; i) M1·CuI, K₂CO₃, THF, 15 h, 60 °C; M2, [Cu(MeCN)₄][PF₆], i-Pr₂NEt, CHCl₃, 18 h, 60°C; ii) TBAF, THF, 30 min, 20°C; iii) M1: CuCl, TMEDA, CH₂Cl₂, 30 min, 20°C, O₂; M2: CuCl, 4,4'-di-t-butyl-2,2'-bipyridine, CH₂Cl₂, 20 h, 30 °C, O_2 ; iv) M1: I_2 , THF, 3 h, 20 °C, M2: I_2 , THF, MeCN (1:1 ν/ν), 5 min, 20 °C.

followed by slow evaporation of the solvent. Despite considerable efforts, it was only possible to grow poor quality crystals that were highly unstable to solvent loss. The structure has four 4:M1 rotaxane moieties in the asymmetric unit and there is significant disorder, contributing to an absence of high-resolution data. To ensure sensible displacement parameters and that the local geometry remained feasible, restraints were required, so it is not possible to compare derived parameters in detail. In spite of this, it is clear that all four molecules have similar geometries, with the PPh₂CH₂PPh₂ ligand oriented towards the TIPS group, away from the polyyne, so that the macrocycle is buttressed by four carbonyl groups at one face and by the three t-Bu groups of a supertrityl stopper at the other face (Figure 1).

The triisopropylsilyl (TIPS) protecting groups were removed from the [2]rotaxanes 4·M1 and 4·M2 using TBAF in wet THF, then the terminal alkynes 5.M1 and 5.M2 were subjected to Cu-catalyzed oxidative homocoupling to obtain the [3]rotaxanes $6 \cdot (M1)_2$ and $6 \cdot (M2)_2$. To our surprise, the different macrocycles required different reaction conditions for this Glaser coupling step. Standard Glaser-Hay conditions (CuCl, TMEDA, CH2Cl2, O2) cleanly converted **5.M1** to [3]rotaxane $6 \cdot (M1)_2$ in 90% yield. However, the oxidative homocoupling of 5:M2 to afford the nanohoop [3]rotaxane $6 \cdot (M2)_2$ was unexpectedly problematic. Standard Glaser-Hay conditions rapidly convert 5.M2 to unidentified by-products, and we found that the free nanohoop M2 is not stable under these conditions (CuCl, TMEDA, CH₂Cl₂, O₂, 20°C, 30 min). A variety of Cu^I and Cu^I/Pd⁰ mixed catalyst

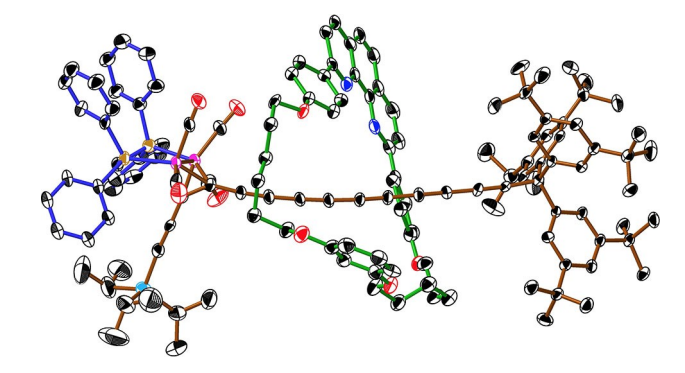


Figure 1. Crystal and molecular structure of [2]rotaxane 4·M1 (one of the four molecules in the asymmetric unit; displacement ellipsoids at 30% probability, hydrogen atoms and minor component of disorder omitted for clarity).

systems were trialed, yet none yielded the expected product. However, successful coupling was observed when using 4,4'di-tert-butyl-2,2'-bipyridine instead of TMEDA under Glaser-Hay coupling conditions. [6b] Warming to 30°C significantly accelerated the reaction, compared with coupling at 20°C (although it is still markedly slower than with TMEDA), and the [3]rotaxane $6 \cdot (M2)_2$ was isolated in 77 % yield after 20 h.

The final polyyne [3]rotaxanes $1 \cdot (M1)_2$ and $1 \cdot (M2)_2$ were prepared by oxidative decomplexation of the corresponding masked [3]rotaxanes using iodine. Once again, the two rotaxanes 6·(M1)₂ and 6·(M2)₂ varied significantly in reactivity. In the case of 6·(M1)2, unmasking proved capricious. Even after meticulous optimization of the reaction conditions, the polyyne rotaxane $1\cdot(M1)_2$ could only rarely be obtained in yields of 20-36%. In contrast, treatment of [3] rotaxane $6 \cdot (M2)_2$ with iodine in a 1:1 THF/MeCN reliably gave polyyne [3]rotaxane 1·(M2)₂ in 32% isolated yield. Both [3]rotaxanes $1 \cdot (M1)_2$ and $1 \cdot (M2)_2$ are stable under ambient conditions, both as solids and in solution over a period of weeks (monitored by UV/Vis spectroscopy).

The ¹H and ¹³C NMR spectra of the [3]rotaxanes **1·(M1)**₂ and 1·(M2)₂ are similar to the sum of the spectra of their components (1+M1 and 1+M2, respectively; see Supporting Information, Figures S17, S24 and S25), indicating the absence of any strong interaction between the polyyne dumbbell and the macrocycles. The spectra of the nanohoop polyyne [3]rotaxane 1·(M2)₂ reveal that rotation of the paraphenylene units of the threaded nanohoop M2 is slow on the NMR timescale, making the two faces of the nanohoop chemically non-equivalent. Thus 10 distinct para-phenylene C-H environments are observed in the HSQC spectrum of 1·(M2)₂ (Figure 2), whereas the free nanohoop M2 gives only 5 para-phenylene CH signals.

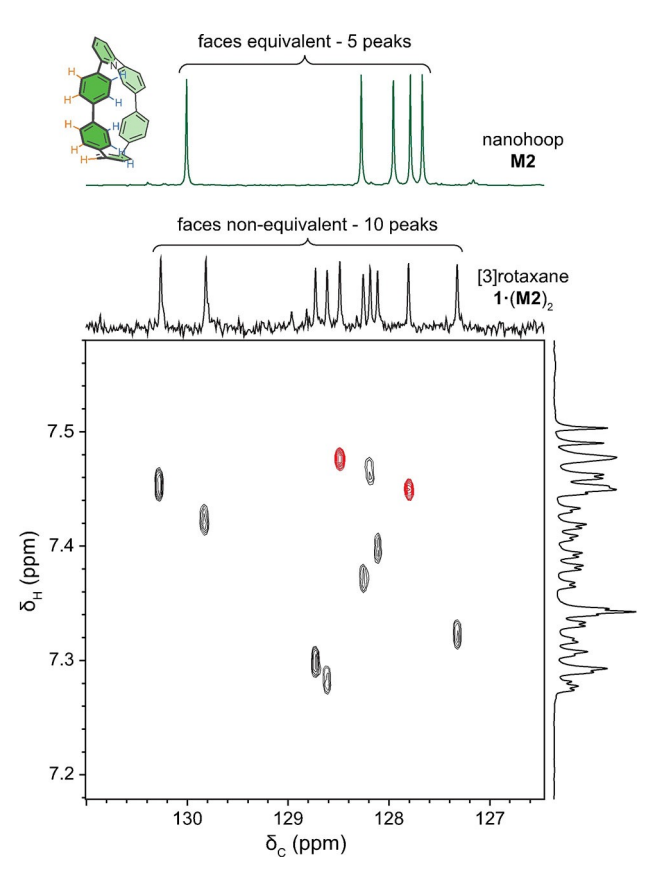


Figure 2. Top: Partial ¹³C NMR spectra of (green) the free nanohoop and (black) the nanohoop-protected polyyne [3]rotaxane 1-(M2)2. Bottom: High-resolution HSQC spectrum showing C-H correlation for the chemically non-equivalent para-phenylene C-H signals. Cross peaks arising from the middle para-phenylene, furthest away from the pyridine unit, have been colored red. The ¹H reference spectrum has been diffusion edited to attenuate the overlapping CHCl₃ resonance (CDCl₃, 298 K, 700 MHz ¹H frequency).

The UV/Vis absorption spectra of 1·(M1), and 1·(M2), (Figure 3) closely resemble the spectrum of the free dumbbell 1, previously reported by Tykwinski et al. [6a] The slight bathochromic shift in the spectra of the [3]rotaxanes (5 nm for M1 and 7 nm for M2) is attributed to the different solvation environments in the [3]rotaxanes. Similar shifts have been reported in the UV/Vis spectra of other polyyne rotaxanes. [8c] Nanohoop M2 is known to be highly fluorescent, [10,16] but its fluorescence is totally quenched in 1·(M2)₂ (see Supporting Information, Figure S27), probably via energy transfer to dark states of the polyyne. [18,19] Thus, although the absorption spectra show only a minimal interaction between the macrocycle and the polyyne in the ground state, there is a significant interaction in the excited

Next we tested whether the chemical stability of the C₂₈ polyyne axle of 1 is enhanced by supramolecular encapsulation. Previously, differential scanning calorimetry (DSC) has been used to demonstrate a stability enhancement in some polyyne rotaxanes.[8c] The problem with studying solid-state stability is that it is influenced by unpredictable crystal packing effects. DSC analysis of 1 and 1·(M2)2 showed that they decompose at similar temperatures (155 °C and 149 °C, respectively, see Supporting Information, Figure S37). We also investigated the stability of these compounds in solution. Oxygen-free solutions of thread 1 and [3]rotaxanes $1\cdot(M1)_2$ and $1\cdot(M2)_2$ in decalin, at a concentration of about 1 μM, were heated to 80 °C in a silica cuvette and decomposition was monitored by UV/Vis spectroscopy. The sharp UV bands of the polyyne were found to decay exponentially, consistent with first-order reaction kinetics (Figure 4). Fitting these data gave apparent first-order rate constants of $0.092~s^{-1},~0.080~s^{-1}$ and $0.021~s^{-1}$ for the dumbbell 1 and the phenanthroline and nanohoop [3]rotaxanes 1·(M1)₂ and 1·(M2)₂, respectively. Experimental uncertainties associated with these measurements were estimated from repeat experiments at approximately 10%. The minimal stability

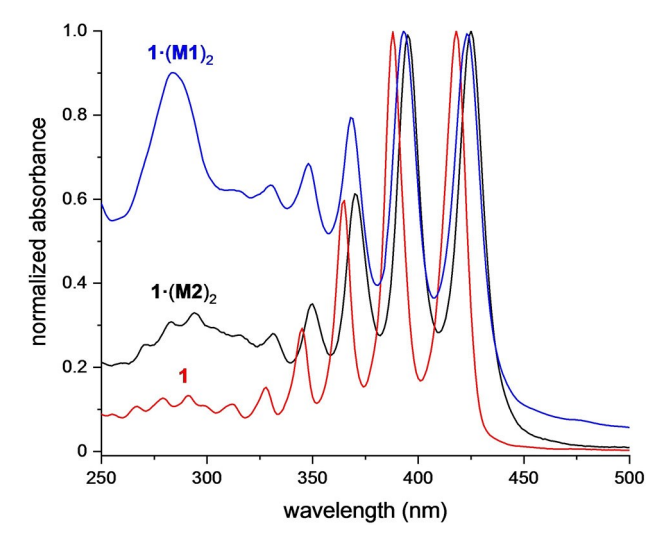


Figure 3. Normalized UV/Vis absorption spectra of polyyne 1 (red), phenanthroline [3]rotaxane 1·(M1)2 (blue) and nanohoop [3]rotaxane $1 \cdot (M2)_2$ (black), all as solutions in *n*-hexane at 25 °C.

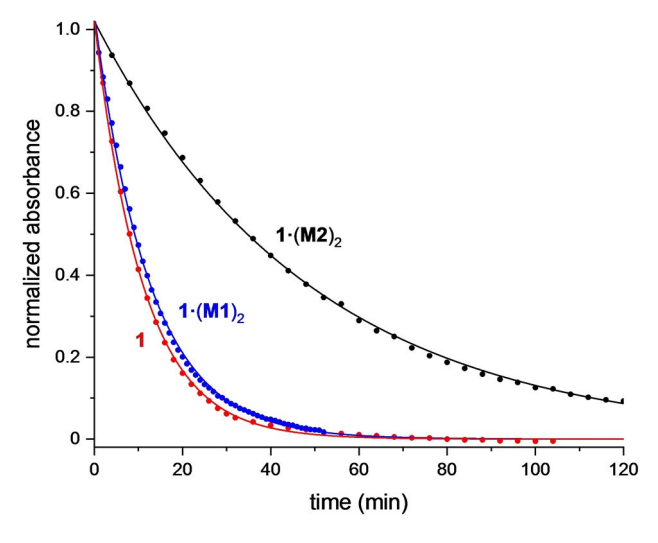


Figure 4. Thermal decomposition of the polyyne dumbbell 1 (red), phenanthroline [3]rotaxane 1·(M1)2 (blue) and nanohoop [3]rotaxane 1.(M2)2 (black) (decalin, 80°C). The intensity of lowest energy band (418 nm, 423 nm and 425 nm for dumbbell 1 and [3]rotaxanes 1·(M1)₂ and 1·(M2)2, respectively) was followed in each case. Data are fitted to a first-order exponential decay; normalized absorbance =- $(A-A_f)/(A_0-A_f) = \exp(-kt)$, where A, A_0 and A_f are the absorbance at time t, absorbance at t=0 and absorbance at $t=\infty$, respectively, and k is the rate constant; see details in Supporting Information.

enhancement for 1·(M1)2 may be attributed to the greater size and flexibility of the phenanthroline macrocycle, which does not effectively shield the polyyne. The tighter nanohoop in 1:(M2)2 enhances the stability of the threaded polyyne by a factor of approximately 4.5.

In summary, we have presented a new synthetic route to polyyne [3]rotaxanes, and we have shown that the size and shape of the macrocycle influence its ability to enhance the thermal stability of a threaded polyyne. Frauenrath et al. reported a [3]rotaxane consisting of a hexayne dumbbell threaded through two cyclodextrin rings, which also exhibited dramatic stability enhancement. [20] Their synthesis used hydrophobic binding to promote threading, which required the [3]rotaxane to be prepared in aqueous solution. Active metal template coupling is a more versatile approach to polyyne rotaxanes, and the ability to prepare polyrotaxanes with cylindrical nanohoop macrocycles is a significant step towards the synthesis of encapsulated carbyne.

Acknowledgements

This project was funded by Leverhulme Trust project grant RPG-2017-032 and the EPSRC. P.G. was supported by Swiss National Science Foundation Postdoc. Mobility fellowship P300P2-177829. R.J. and C.E.O. were supported by the National Science Foundation (CHE-1808791). We thank Dr. Jeffrey M. Van Raden, Dr. Yueze Gao and Dr. Steffen L. Woltering for valuable discussion.

Conflict of Interest

The authors declare no conflict of interest.

Data Availability Statement

The data that support the findings of this study are available in the supplementary material of this article.

Keywords: Rotaxanes · Acetylene · Polyynes · Thermal Stability · Template-Directed Synthesis

- [1] a) E. Arunkumar, C. C. Forbes, B. D. Smith, Eur. J. Org. Chem. 2005, 4051-4059; b) M. J. Frampton, H. L. Anderson, Angew. Chem. Int. Ed. 2007, 46, 1028-1064; Angew. Chem. **2007**, 119, 1046–1083; c) S. Brovelli, F. Cacialli, Small **2010**, 6, 2796-2820; d) H. Masai, J. Terao, Polymer 2017, 49, 805-814; e) J. Royakkers, H. Bronstein, Macromolecules 2021, 54, 1083-1094.
- [2] a) F. Cacialli, J. S. Wilson, J. J. Michels, C. Daniel, C. Silva, R. H. Friend, N. Severin, P. Samorì, J. P. Rabe, M. J. O'Connell, P. N. Taylor, H. L. Anderson, Nat. Mater. 2002, 1, 160-164; b) M. M. Mróz, G. Sforazzini, Y. Zhong, K. S. Wong, H. L. Anderson, G. Lanzani, J. Cabanillas-Gonzalez, Adv. Mater. 2013, 25, 4347-4351; c) T. Ohto, H. Masai, J. Terao, W. Matsuda, S. Seki, Y. Tsuji, H. Tada, J. Phys. Chem. C 2016, 120, 26637-26644.
- [3] a) J. E. H. Buston, J. R. Young, H. L. Anderson, Chem. Commun. 2000, 905-906; b) M. R. Craig, M. G. Hutchings, T. D. W. Claridge, H. L. Anderson, Angew. Chem. Int. Ed. 2001, 40, 1071-1074; Angew. Chem. 2001, 113, 1105-1108; c) E. Arunkumar, N. Fu, B. D. Smith, Chem. Eur. J. 2006, 12, 4684-4690; d) H. O. Bak, B. E. Nielsen, M. Å. Petersen, A. Jeppesen, T. Brock-Nannestad, C. B. O. Nielsen, M. Pittelkow, New J. Chem. 2020, 44, 20930-20934.
- a) F. Diederich, Nature 1994, 369, 199-207; b) R. R. Tykwinski, Chem. Rec. 2015, 15, 1060-1074; c) P. Tarakeshwar, P. R. Buseck, H. W. Kroto, J. Phys. Chem. Lett. 2016, 7, 1675-1681; d) C. S. Casari, A. Milani, MRS Commun. 2018, 8, 207-219; e) F. Banhart, ChemTexts 2020, 6, 3.
- [5] L. Shi, P. Rohringer, K. Suenaga, Y. Niimi, J. Kotakoski, J. C. Meyer, H. Peterlik, M. Wanko, S. Cahangirov, A. Rubio, Z. J. Lapin, L. Novotny, P. Ayala, T. Pichler, Nat. Mater. 2016, 15, 634-640.
- [6] a) W. A. Chalifoux, R. R. Tykwinski, Nat. Chem. 2010, 2, 967-9714; b) Y. Gao, Y. Hou, F. G. Gámez, M. J. Ferguson, J. Casado, R. R. Tykwinski, Nat. Chem. 2020, 12, 1143-1149.
- [7] a) S. Saito, E. Takahashi, K. Nakazono, Org. Lett. 2006, 8, 5133-5136; b) J. Berná, J. D. Crowley, S. M. Goldup, K. D. Hänni, A.-L. Lee, D. A. Leigh, Angew. Chem. Int. Ed. 2007, 46, 5709-5713; Angew. Chem. 2007, 119, 5811-5815.
- [8] a) L. D. Movsisyan, D. V. Kondratuk, M. Franz, A. L. Thompson, R. R. Tykwinski, H. L. Anderson, Org. Lett. 2012, 14, 3424-3426; b) N. Weisbach, Z. Baranova, S. Gauthier, J. H. Reibenspies, J. A. Gladysz, Chem. Commun. 2012, 48, 7562-7564; c) L. D. Movsisyan, M. Franz, F. Hampel, A. L. Thompson, R. R. Tykwinski, H. L. Anderson, J. Am. Chem. Soc. 2016, 138, 1366-1376.
- [9] a) S. L. Woltering, P. Gawel, K. E. Christensen, A. L. Thompson, H. L. Anderson, J. Am. Chem. Soc. 2020, 142, 13523-13532; b) P. Gawel, S. L. Woltering, Y. Xiong, K. E. Christensen, H. L. Anderson, Angew. Chem. Int. Ed. 2021, 60, 5941-5947; Angew. Chem. 2021, 133, 6006-6012.

Communications



- [10] J. M. Van Raden, B. M. White, L. N. Zakharov, R. Jasti, Angew. Chem. Int. Ed. 2019, 58, 7341–7345; Angew. Chem. 2019, 131, 7419–7423.
- [11] D. R. Kohn, P. Gawel, Y. Xiong, K. E. Christensen, H. L. Anderson, J. Org. Chem. 2018, 83, 2077–2086.
- [12] a) Y. Rubin, C. B. Knobler, F. Diederich, J. Am. Chem. Soc. 1990, 112, 4966–4968; b) M. M. Haley, B. L. Langsdorf, Chem. Commun. 1997, 1121–1122.
- [13] M. J. Langton, J. D. Matichak, A. L. Thompson, H. L. Anderson, *Chem. Sci.* **2011**, 2, 1897–1901.
- [14] a) S. Eisler, R. R. Tykwinski, J. Am. Chem. Soc. 2000, 122, 10736–10737; b) S. Eisler, N. Chahal, R. McDonald, R. R. Tykwinski, Chem. Eur. J. 2003, 9, 2542–2550.
- [15] M. Franz, J. A. Januszewski, F. Hampel, R. R. Tykwinski, Eur. J. Org. Chem. 2019, 3503–3512.
- [16] J. M. Van Raden, N. N. Jarenwattananon, L. N. Zakharov, R. Jasti, Chem. Eur. J. 2020, 26, 10205–10209.
- [17] Single-crystal X-ray diffraction data for 4-M1 were collected using a (Rigaku) Oxford Diffraction SuperNova diffractometer at 150 K. Raw frame data were reduced using CrysAlisPro and the structure was solved using SuperFlip [a) L. Palatinus, G. Chapuis, J. Appl. Crystallogr. 2007, 40, 786–790] before refinement with CRYSTALS [b) P. Parois, R. I. Cooper, A. L. Thompson, Chem. Cent. J. 2015, 9, 30; c) R. I. Cooper, A. L.
- Thompson, D. J. Watkin, *J. Appl. Crystallogr.* **2010**, *43*, 1100–1107]. On initial refinement, many of the terminal atoms were found to display prolate displacement ellipsoids thought to be caused by disorder; these were treated with a split site model, but the poor signal to noise and lack of high angle data meant restraints were needed. For further details see the Supporting Information (CIF). d) Crystallographic data have been deposited with the Cambridge Crystallographic Data Centre (2127806) and can be obtained via https://www.ccdc.cam.ac.uk/structures/.
- [18] a) L. D. Movsisyan, M. D. Peeks, G. M. Greetham, M. Towrie,
 A. L. Thompson, A. W. Parker, H. L. Anderson, *J. Am. Chem. Soc.* 2014, 136, 17996–18008; b) D. R. Kohn, L. D. Movsisyan,
 A. L. Thompson, H. L. Anderson, *Org. Lett.* 2017, 19, 348–351.
- [19] J. Zirzlmeier, S. Schrettl, J. C. Brauer, E. Contal, L. Vannay, É. Brémond, E. Jahnke, D. M. Guldi, C. Corminboeuf, R. R. Tykwinski, H. Frauenrath, *Nat. Commun.* 2020, 11, 4797.
- [20] S. Schrettl, E. Contal, T. Hoheisel, M. Fritzsche, S. Balog, R. Szilluweit, H. Frauenrath, *Chem. Sci.* 2015, 6, 564–574.

Manuscript received: December 10, 2021 Accepted manuscript online: January 7, 2022 Version of record online: January 20, 2022